Journal of Inorganic and Organometallic Polymers and Materials (2018) 28:2069–2079
https://doi.org/10.1007/s10904-018-0893-9

Physical Crosslinked Poly(*N*-isopropylacrylamide)/Nano-Hydroxyapatite Thermosensitive Composite Hydrogels

Shuo Wang[1] · Zhaofu Zhang[1] · Qihai Zhang[2] · Lifang Li[1]

Received: 28 February 2018 / Accepted: 6 June 2018 / Published online: 6 July 2018

Abstract
Injectable and thermosensitive poly(*N*-isopropylacrylamide) (PNIPA)/nano-hydroxyapatite (nano-HA) composite hydrogels were synthesized by physical crosslinking of *N*-isopropylacrylamide with nano-HA as cross-linker to improve the mechanical property of hydrogels and avoid the use of chemical cross-linker. Internal morphology, thermosensitive, rheological, swelling, and hemocompatibility properties of the prepared hydrogels were investigated. The PNIPA/HA composite hydrogels had a phase transition from sol to gel, and the lowest critical solution temperature was about 32.5 °C. The PNIPA/HA composite hydrogels had regular pore structures and the nano-HA dispersed well throughout the network. Differential scanning calorimetry and thermogravimetric analysis showed that the addition of nano-HA had no significant effect on the LCST and thermal stability of the PNIPA/HA hydrogels. When the temperature was above 32.5 °C, the storage modulus (*G′*) and complex viscosity increased with the increasing nano-HA content. All PNIPA/HA composite hydrogels possessed the thinning behavior. The PNIPA/HA hydrogels exhibited a good water absorption capacity and the swelling ratio decreased with the increasing nano-HA content. As revealed by biocompatibility results, PNIPA/HA composite hydrogels were considered to be a non-hemolytic biomaterial. Therefore, PNIPA/HA hydrogels can be used as injectable materials for the potential applications of science and technology, such as tissue engineering scaffolds.

Keywords *N*-Isopropyl acrylamide · Nano-hydroxyapatite · Thermosensitive composite hydrogels · Hemocompatibility · Injectable materials

1 Introduction

Natural bone is a composite material made up of the collagen and hydroxyapatite (HA) [$Ca_{10}(PO_4)_6(OH)_2$] crystals which account for 2/3 of the bone weight [1, 2]. As a kind of typical biological material with excellent biocompatibility and bioactivity, HA is often used as bone regeneration [3], drug carrier [4] and artificial materials [5]. Moreover, HA display excellent characteristics, such as high surface energy, to enhance and maintain mechanical properties of the composite or polymeric materials [6–8]. The HA/polymer composite materials have become a research hot spot in nowadays, and present studies of HA/polymer composite materials are main focused on the area of bone tissue engineering [9–11].

Hydrogels composed by polymeric chains and water possess tridimensional networks. They can absorb large amounts of water and swell to maintain its original structure. Traditionally, they display special properties such as sensitive responses to environments, hydrophilic nature and adequate viscoelasticity. Smart hydrogels can undergo volume or phase transition in sensitive response to environmental stimuli including temperature [12], pH [13], electric field [14] and light [15]. Attributed to their sensitive responses, smart hydrogels are widely applied in tissue engineering, drug delivery, and bio-separation [16–20].

One of the most intensively studied hydrogels is constructed by thermosensitive polymers which exhibit phase-separation changes when the temperature varies [21].

✉ Qihai Zhang
zhqh816@163.com

✉ Lifang Li
fangll@sdau.edu.cn

[1] College of Chemistry and Material Science, Shandong Agricultural University, 61 Daizong Street, Tai′an, Shandong 271018, People's Republic of China

[2] Department of Pediatric Orthopedics, Tai'an Central Hospital, Tai'an, Shandong 271000, People's Republic of China

Thermal shrinkage and expansion hydrogels are typical behaviors for thermosensitive hydrogels. Thermally shrinkable hydrogels are soluble at low temperatures and become insoluble with the temperature is increased above the lower critical solution temperature (LCST) [22]. Poly(*N*-isopropylacrylamide) (PNIPA) has attracted increasing attention since Scarpa investigated the phase transition heat of PNIPA [23]. NIPA as the monomer of PNIPA has unique molecular structure including both hydrophilic amide group and hydrophobic isopropyl groups. Isopropyl group and carbon chains form the skeleton of the NIPA molecule, and the amide group forms a strong hydrogen bond, which enhances its hydrophilicity ability in the aqueous phase. Heskins and Guillet first reported that the thermosensitive property of PNIPA and the LCST of PNIPA was 32 °C [24]. Below its LCST, the amide bonds and water will form hydrogen bonds. While the isopropyl and hydrocarbon skeleton can form hydrophobic groups by the hydrophobic association. PNIPA hydrogels exhibit thermosensitive swelling properties with a transform of sol to gel [25], and it is widely used in various fields of life science technology and bioengineering such as cell culture [26], enzymes immobilization [27], controlled drugs and gene delivery [28], bone tissue engineering [29], and separation technology [30].

Physically and chemically crosslinked hydrogels are the most commonly used methods for the preparation of hydrogels [31]. So far, PNIPA composite hydrogels have been commonly prepared by conventional chemical method with NIPA as monomer, persulfate as initiator, and chemical crosslinking agent as cross-linker [32]. The initiator and chemical crosslinking agent are important for the response rate of hydrogels, however, their residuals will lead to the toxicity and limit the applications of materials in many biological fields. Chemically crosslinked hydrogels are usually swellable with no phase transition, and they have network structures forming a bulk polymer. Physically crosslinked hydrogels are mostly formed through the weak hydrophobic interactions between hydrocarbon chains and hydrogen bonds or ionic bonds between the hydrophilic groups, leading to the formation of a linear polymer, and the strength is relatively weak when it transforms from sol to gel. The combination of bioactive inorganic materials and organic elastomers is a prevailing strategy to overcome the shortcomings mentioned above and the poor stability of organic macromolecules, and the composites are endowed with excellent performance in mechanical and thermal properties, as well as the stability [33–35]. HA is one of the excellent inorganic biological materials with low toxicity and it has spherical or rod-like structure. When HA is used as the crosslinking agent, the asymmetric structure will have a better cross-linking strength. Based on these, in present study nano-hydroxyapatite (nano-HA) with larger axial diameter and better cross-linking effect was applied as physical crosslinking agent to form thermosensitive PNIPA/HA organic–inorganic composite hydrogels. Also, the use of nano-HA avoids the introduction of toxic and organic chemicals. Interestingly, the composite exhibited good thermosensitivity and excellent mechanical properties, which provide the potential for the application in tissue engineering using as injectable materials.

2 Experimental

2.1 Materials

N-Isopropylacrylamide (stabilized with hydroquinone monomethylether) (NIPA) and calcium nitrate tetrahydrate [$Ca(NO_3)_2{\cdot}4H_2O$] were purchased from TCI and BASF company, respectively. Diammonium hydrogen phosphate [$(NH_4)_2HPO_4$], ammonia ($NH_3{\cdot}H_2O$) and anhydrous ethanol (C_2H_5OH) were provided from Tianjin Kaitong Chemical Reagent Co., Ltd. Besides, Potassium persulfate (KPS) and tetramethylethylenediamine (TEMED) were obtained from Aladdin Industrial Corporation. Polyvinylpyrrolidone K30 (PVP-K30) was supplied by Shanghai Boao Biotechnology Co. Ltd. Normal saline (NS) was obtained from Cisen Pharmaceutical Co., Ltd., and the red blood was taken from healthy adults. All the chemicals were used as received without further purification. Redistilled water and distilled water were used in the experimentation.

2.2 Synthesis of Nano-HA

The nano-HA was prepared through co-precipitation method using $Ca(NO_3)_2{\cdot}4H_2O$ and $(NH_4)_2HPO_4$ as Ca and P precursors (at molar ratio $Ca/P \geq 1.67$). The crystallization process of nano-HA was achieved by controlling the reaction temperature, pH, and reaction time.

The $(NH_4)_2HPO_4$ solution was added drop by drop into the $Ca(NO_3)_2{\cdot}4H_2O$ solution within 2 h. The mass fraction of PVP K30 as a surfactant to the total quality was 2%. After the first step, the white precipitate was dried. Appropriate amount of the dried corresponding precipitate was dispersed in distilled water to aging with 100 °C for 12 h. The minimum pH was adjusted to 10 by adding $NH_3{\cdot}H_2O$. After aging, the obtained white precipitate was filtered, and washed three to four times with distilled water and anhydrous ethanol until the complete removal of ammonium nitrate. Finally, the precipitate was centrifuged at medium speed (3000 rpm min^{-1}) for 10 min and then dried at 80 °C for 24 h.

2.3 Synthesis of PNIPA Organic–Inorganic Composite Hydrogels

PNIPA composite hydrogels were prepared by the radical polymerizations as shown in Scheme 1. For each polymerization, 0.3 g NIPA was dissolved in 6 mL distilled water at 25 °C. A certain amount of nano-HA was also added to the solution. 0.01 g potassium persulfate (KPS) and 6 μL TEMED were then added into the mixed system as the initiator and accelerator to initiate the polymerization. The samples were dispersed completely under the assistant of low temperature ultrasound for 2–4 min. The polymerization was carried out at 25 °C and lasted for 15 h under a nitrogen atmosphere. The quality ratios of m_{HA}/m_{NIPA} were changed into 0, 2, 3, 4, 5‰, and the corresponding hydrogel samples were denoted as PNIPA-0, PNIPA/HA-2, PNIPA/HA-3, PNIPA/HA-4 and PNIPA/HA-5. The composite hydrogels were immersed in deionized water for 24 h and then washed three times to remove unreacted monomers.

2.4 Characterization

The gelation of the composite hydrogels was observed at 20 and 40 °C. Prepared PNIPA/HA composite hydrogels were frozen in a refrigerator (Zhongke Meiling Instrument Co., Ltd.) at − 20 °C for 4 h and − 80 °C for 10 h. Then the samples were freeze-dried in a Freeze Drier (Beijing boyikang Lab Instrument Co., Ltd.) under vacuum at − 80 °C for at least 24 h until all the solvents were sublimed. The freeze-dried samples were cut into small pieces for further use.

2.4.1 X-ray Diffraction Analysis (XRD)

The wide-angle X-ray diffraction data over the 2θ range from 20° to 60° of nano-HA were measured using an X-ray diffractometer (PW3710, Philips) with a Cu tube anode.

2.4.2 Fourier Transform Infrared Spectrum (FT-IR)

The presence of the expected functional groups associated to the presence of NIPA and nano-HA in the PNIPA/HA composite hydrogels was confirmed by fourier transform infrared spectrometer (Nicolet 380, Thermo Fisher Scientific Inc., America) in a KBr flake.

2.4.3 Scanning Electron Microscopy (SEM)

The fracture surface morphology of the composite hydrogels was analyzed by a scanning electron microscope (Merlin compact, Carl Zeiss AG) operated at 20 kV. The samples were broken off after frozen in liquid nitrogen.

2.4.4 Differential Scanning Calorimetry (DSC)

The thermal behavior or LCST behaviors of the hydrogels were determined using a differential scanning calorimeter (Q80, DSC, TA instruments, America). DSC experiments were performed on swollen hydrogel specimens of 10 mg by heating from 20 to 40 °C at a heating rate of 5 °C min^{-1} under nitrogen flow.

2.4.5 Thermal Stability (TGA)

The thermal stability of the composite hydrogels was analyzed by thermogravimetric analyses (DTG-60 A, Shimadzu, Japan). The composite hydrogels were measured from 30 to 600 °C at a heating rate of 20 °C min^{-1} with samples mass (5–10 mg) under nitrogen atmosphere (50 mL min^{-1}).

2.4.6 Rheological Measurements

Rheological studies were carried out using a DHR rotational rheometer (TA. Inc., America). All studies were carried out using a stainless steel 40 mm cone plate (2°) (upper), and the gap between the upper and lower plates was kept at 53 mm. The temperature was maintained at 25 °C. Amplitude sweep was carried out from a strain percentage of 10^{-1}, and the

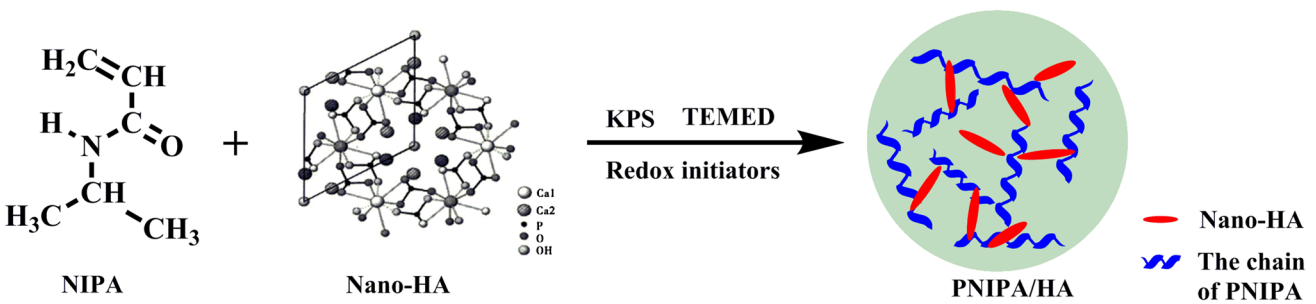

Scheme 1 Preparation of PNIPA/HA composite hydrogels

instrument was set to automatically determine the end of the linear viscoelastic region (LVER). The following experiment was carried out in the linear viscoelastic region of PNIPA/HA composite hydrogels.

The hydrogels were subjected to different temperature ranging from 25 to 40 °C under constant angular frequency (10 rad s^{-1}) and shear strain (5%), and the complex modulus and complex viscosity were measured. This test was to measure the stability of the PNIPA/HA composite hydrogels from room temperature to normal body temperature.

The viscosities of the control and composite hydrogels were plotted against varying shear rates of 10^{-1}–10^{3} s^{-1} to obtain the flow curves. The temperature was maintained at 25 °C. The rheological curve analysis can be used to predict the injection ability of hydrogels.

2.4.7 Swelling Studies

The swelling studies were carried out in 5 mL normal saline (NS, 0.9%) solution at 37 °C without shaking and stirring. The freeze-dried samples were weighed first and then immersed in NS solution until they swelled to equilibrium. At a predetermined time, the swollen samples were taken out to remove the excessive surface water with filter paper and then weighed. The swelling ratio (SR) was calculated by the equation:

$$\mathrm{SR}\ (\%) = \frac{W_t - W_d}{W_d} \times 100\%$$

where W_t is the weight of swollen hydrogels at 37 °C, and W_d is the weight of dry hydrogels.

2.4.8 Hemolysis Assay

The hemolytic activity of the hydrogels was determined by contact methods. 2.5 mL of the whole blood (taken from healthy adults) was added to 2.5 mL NS solution to which 0.3 mL of the four samples had been added. The NS solution and distilled water were used as the negative and the positive control, respectively. All the samples were put in the centrifuge tubes, and then the contents of the tubes were gently mixed and incubated in 37 °C for 3 h. Subsequently, the samples were centrifuged at 1500 rpm for 5 min, and the absorbance of the supernatant liquid in each tube was determined at 540 nm, using a UV/Vis spectrophotometer (UV-2450, Shimadzu, Japan). The hemolysis rate is calculated according to the following formula:

$$\mathrm{HR}\ (\%) = \frac{A_{sample} - A_{negative}}{A_{positive} - A_{negative}} \times 100\%$$

where A_{sample} is the absorbance of each sample, $A_{negative}$ is the absorbance of the negative control, and $A_{positive}$ is the absorbance of the positive control.

3 Results and Discussion

3.1 Macro Analysis of Composite Hydrogels

In the process of the composite hydrogels synthesis, it was found that when the nano-HA content was deeply low ($0 < m_{HA}/m_{NIPA} < 2‰$), no crosslinking occurred in the composite hydrogels. While the nano-HA content increased to $m_{HA}/m_{NIPA} > 5‰$, the composite hydrogels were illiquid and the viscoelastic modulus of composite hydrogels were so high beyond the measurement range of the instrument. Therefore, the PNIPA-0, PNIPA/HA-2, PNIPA/HA-3, PNIPA/HA-4 and PNIPA/HA-5 were selected for subsequent characterization.

It was found that the samples had similar morphologies below and above its LCST (about 32.5 °C), so the temperature of 20 and 40 °C were chosen as a typical representation of being lower or higher than LCST. The photos are shown in Fig. 1. Obviously, it can be seen that both hydrogels

Fig. 1 Visual aspect of PNIPA-0, PNIPA/HA-2 hydrogels at 20 and 40 °C

maintained good fluidity at 20 °C. When the temperature raised to 40 °C, the PNIPA/HA-2 sample turned into opaque and illiquid. However, the PNIPA-0 hydrogel could not be coagulated like other hydrogels, only some white precipitation occurred. The reason for this discrepancy might be that the elevated temperature (> LCST) excited hydrophobic interaction between isopropyl groups and carbon chains, inducing the hydrophilic ability to decline [36–38], causing partial entanglement in PNIPA-0 sample. But for PNIPA/HA composite hydrogels, the decreased hydrophilicity of amide groups caused the weaken interaction between PNIPA and water molecule [36–38], thereby PNIPA could be absorbed by nano-HA though hydrogen bonding, inducing the formation of hydrogel network. It is a fact that the phase separation at the LCST depends on the arrangement of water molecules around the hydrophobic residues of the PNIPA polymer chains [38], so the hydrophobization of the hydrogel can be explained considering the removal of water molecules around isopropylacrylamide groups due to hydrogen bonding between the amide proton and the surface phosphate ions of nano-HA [39]. Therefore, it can be confirmed that nano-HA can be a cross-linking agent in PNIPA/HA hydrogels. The results shown that the process of heating and cooling could be carried out many times and composite hydrogels restored to the original state. So the obtained PNIPA/HA composite hydrogels were reversible hydrogels.

In view of the results, we illustrated the space structure of PNIPA/HA composite hydrogels at 40 °C (Fig. 2). The nano-HA particles acting as physical cross-linker were crosslinked with PNIPA chains to form hydrogels network. In PNIPA/HA composite hydrogels, the amide proton and the surface phosphate ions of nano-HA formed hydrogen bonds. It might be the presence of hydrogen bonds, meanwhile, both hydrophobic interaction between hydrophobic groups and van der waals attraction contributed to the formation of hydrogels with 3D networks [36–38].

3.2 Structural Analysis of Composite Hydrogels

XRD spectrum of nano-HA has shown in Fig. 3. The crystalline peaks at 25.9°, 31.8°, 32.0°, 33.0° and 40.0° revealed a structure of monophase crystals of nano-HA, which can be determined by comparing the XRD patterns with JCPDS file (No. 9-0432). The peaks of pure nano-HA around 25.9° and 31.8° are (002) and (211) diffraction directions of crystals. The characteristic and sharp diffraction peaks demonstrated the conformation of nano-HA with good single crystal structure.

Figure 4 presents the typical FT-IR spectra of PNIPA/HA (a) composite hydrogels, (b) NIPA, and (c) nano-HA. In Fig. 4c, the peaks at 3455 and 635 cm^{-1} were attributed to the presence of hydroxyl group (–OH) stretching, the characteristic peaks at 1094 and 1030 cm^{-1} were assigned to the typical stretching bonds of P–O and P=O in PO_4^{3-}. In Fig. 4b, there were a clearly amide I bond at 1653 cm^{-1} consisting of the C=O stretching and the amide II bond at 1550 cm^{-1} consisting of the N–H stretching. In addition, the peaks at 1247 cm^{-1} was attributed to the amide III bond stretching of N–H. The peaks at 1395 and 2928 cm^{-1} were assigned to the presence of isopropyl [$–CH(CH_3)_2$] stretching and $–CH_3$ asymmetric stretching. The characteristic peaks seen at 3300 cm^{-1} was assigned to the secondary amide N–H bond. The peaks at 1455 and 1200 cm^{-1} were attributed to the bending of $–CH_3$, $–CH_2$, and –CH.

A comparison of FT-IR spectra of PNIPA/HA composite hydrogels (Fig. 4c) confirmed the existence of nano-HA. The analysis of the characteristic bonds of NIPA in PNIPA/

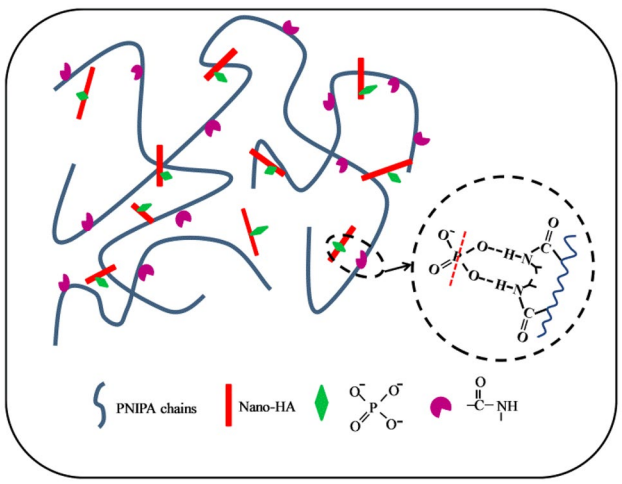

Fig. 2 Simplified illustration of the molecule structure of hydrogels at 40 °C

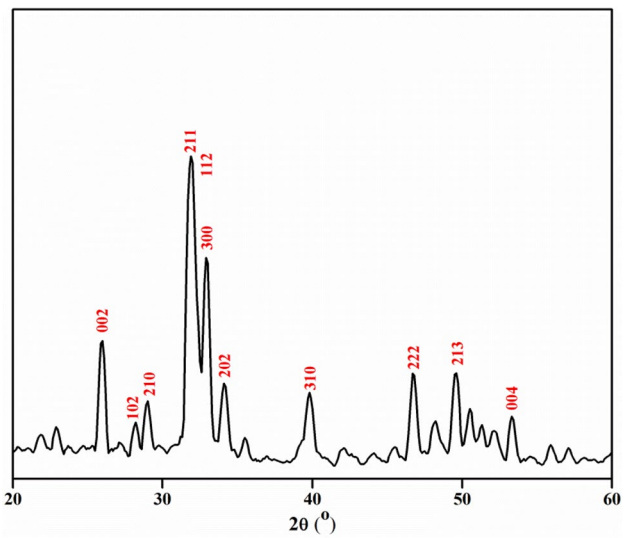

Fig. 3 XRD spectrum of nano-HA

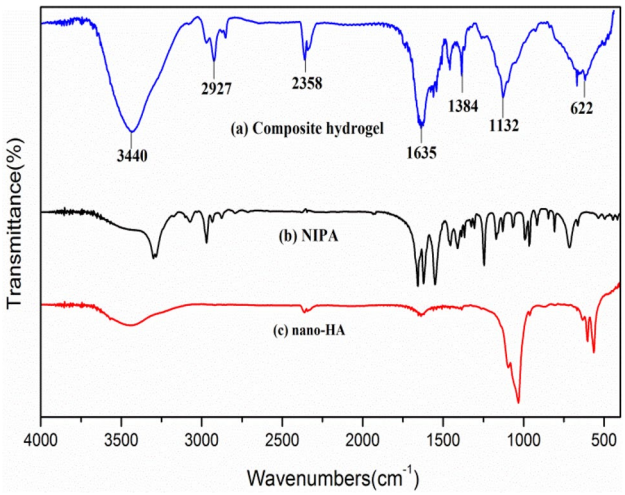

Fig. 4 FT-IR spectra of *a* composite hydrogel, *b* NIPA and *c* nano-HA

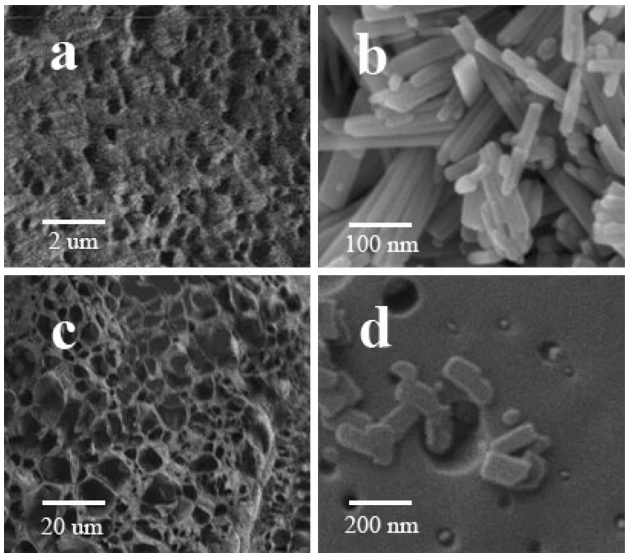

Fig. 5 SEM images of the fracture surfaces of **a** PNIPA-0, **b** nano-HA, **c, d** PNIPA/HA composite hydrogels

HA composite hydrogels spectrum, the bond at 1626 cm^{-1} (in NIPA) was changed to 1635 cm^{-1} (in PNIPA/HA). The bond shifts towards higher wavenumbers and the instanced of peak intensity at the 3440 cm^{-1} might be the effect of the intermolecular hydrogen bonding between NIPA and nano-HA. The absorption peaks of C–H bond at 2927 and 2358 cm^{-1} increased, which were consistent with the formation of the C–H stretching. These changes observed in the spectrum of PNIPA/HA composite hydrogels might be related to the formation of weaker hydrogen bonding.

3.3 SEM Observations of Composite Hydrogels

To study the microstructures of the freeze-dried composite hydrogels samples, SEM is performed as shown in Fig. 5. It can be clearly seen that the PNIPA-0 hydrogel (Fig. 5a) had little hole on its surface. The shape of nano-HA was rod-like structure in the range of 200 nm (Fig. 5b). Comparing Fig. 5a, c, d, it was found that the structure of the PNIPA/HA composite hydrogels had more porous network structure than PNIPA-0 hydrogel, and nano-HA was embedded in the NIPA spatial network.

3.4 Differential Scanning Calorimetry (DSC)

The calorimetric curves of PNIPA/HA composite hydrogels are shown in Fig. 6. LCST was the point where the hydrophobic interactions of the isopropyl groups of PNIPA outweigh the hydrophilic nature of the amide groups on the pendant groups [36]. Obviously, there is nearly no changes in heat absorption and emission peak when the temperature was below 32.5 °C. However, all the PNIPA/HA composite hydrogels showed a pronounced endothermic peak at the LCST (33–34 °C). Generally, PNIPA/HA composite hydrogels have a sol to gel transform at around 33 °C. With the increased of nano-HA content, the LCST shows no significant transition.

3.5 Thermogravimetric Analyses (TGA)

The thermal stability and degradation behavior of PNIPA-0, nano-HA and PNIPA/HA composite hydrogels were measured by thermal gravimetric analysis (TGA) and differential thermal gravity (DTG) have shown in Fig. 7. The major data are summarized at Table 1.

In Fig. 7a, the line of nano-HA was basically horizontal, and it was probably due to the evaporation of water which

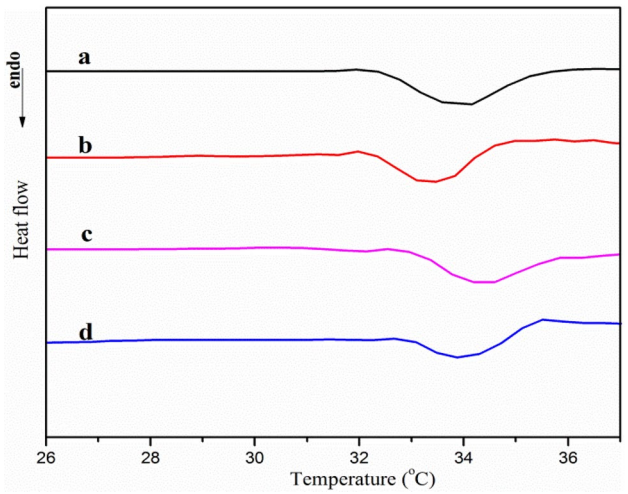

Fig. 6 DSC thermograms of PNIPA/HA composite hydrogels. *a* PNIPA/HA-2, *b* PNIPA/HA-3, *c* PNIPA/HA-4, *d* PNIPA/HA-5

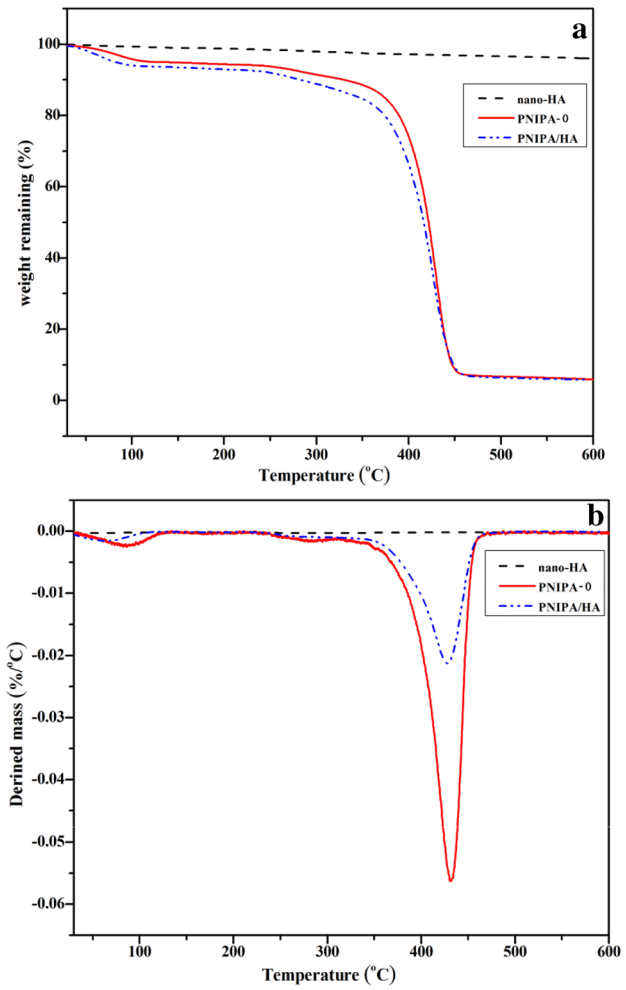

Fig. 7 **a** Thermogravimetric analysis (TGA) and **b** differential thermal gravity (DTG) of PNIPA-0, nano-HA and PNIPA/HA composite hydrogels

Table 1 Major data obtained from TGA and DTG measurements

Sample	$T_{50\%}$ (°C)	$Char_{600}$ (%)	T_{max} (°C)
Nano-HA	–	96.10	–
PNIPA-0	421.54	5.78	432.04
PNIPA/HA	416.30	5.72	428.62

$T_{50\%}$ temperature for 50% weight loss, *Char* char yield, weight of polymer remained, T_{max} maximum decomposition temperature

adsorbed on the surface of nano-HA crystal. There are two steps of weight loss of PNIPA-0 and PNIPA/HA hydrogels. The first step in the range of 50–110 °C was due to the remove of water molecules. It indicated that the samples were not completely dehydrated. And the relative bigger peak in the range of 350–470 °C was probably due to the thermal decomposition of the polymer and splitting of the main chain. For PNIPA-0 and PNIPA/HA hydrogels, it was observed that there was no huge varieties for T_{max}. It indicated that the addition of nano-HA had negligible effect on the T_{max} of the PNIPA/HA composite hydrogels. In addition, the composite hydrogels have shown high thermal resistance (~450 °C).

In Fig. 7b, the T_{max} in weightlessness peak of PNIPA-0 and PNIPA/HA hydrogels were 432.04 and 428.62 °C. The 50% weight loss temperature of PNIPA/HA composite hydrogels was close to that of PNIPA-0, and the hydrogels cannot be decomposed completely when the temperature was raised to 600 °C.

3.6 Rheological Analysis

3.6.1 Viscoelastic Analysis

Viscoelastic analysis was used to find the linear viscoelastic region (LVER) at different oscillation strain. In a linear viscoelastic area, the strain was elastic so that the specimen could restore to its original state once the stress was released. In Fig. 8, it have shown that the PNIPA/HA composite hydrogels with the different contents of nano-HA has similar LVER at 25 °C, which indicates that the addition of nano-HA did not change the viscoelastic behavior of the composite hydrogels. The storage modulus (G') and the loss modulus (G'') changed with the increase of nano-HA content, but G' was always greater than G'', indicating a solid-like and elastic nature of the hydrogels [40]. The state of the hydrogels can be determined by the phase angle (δ). If the phase angle is equal to 0°, it is solid. And the state of the hydrogels will be liquid when the phase angle is equal to 90°. It can be seen that the phase angle of the composite hydrogels had an increasing trend with the addition of nano-HA, which indicates that the composite hydrogels was solid-state and gradually became liquid. The results show the increasing of nano-HA content is beneficial to the formation of well-flowing hydrogel and reduce the viscoelastic modulus slightly. Maybe it is because of the cross-linked effect of nano-HA, which enhance the hydrophilicity of hydrogel.

3.6.2 Study on the Effect of Temperature on Modulus

The moduli of PNIPA/HA composite hydrogels under different temperatures are shown in Fig. 9. The G' and G'' reflects the solid-like and liquid component of the rheological behaviour. The curves are divided into two parts. The first region is below 32 °C, where G'' is lower than G', showing the common viscoelastic behavior of solid-like materials. But the G' and G'' are nearly the same, it indicates that the PNIPA/HA composite hydrogels have both elasticity and viscosity. The possible reason is that when the temperature is lower than LCST, PNIPA is relatively hydrophilic and has a good interaction with water molecules [38]. Therefore, the

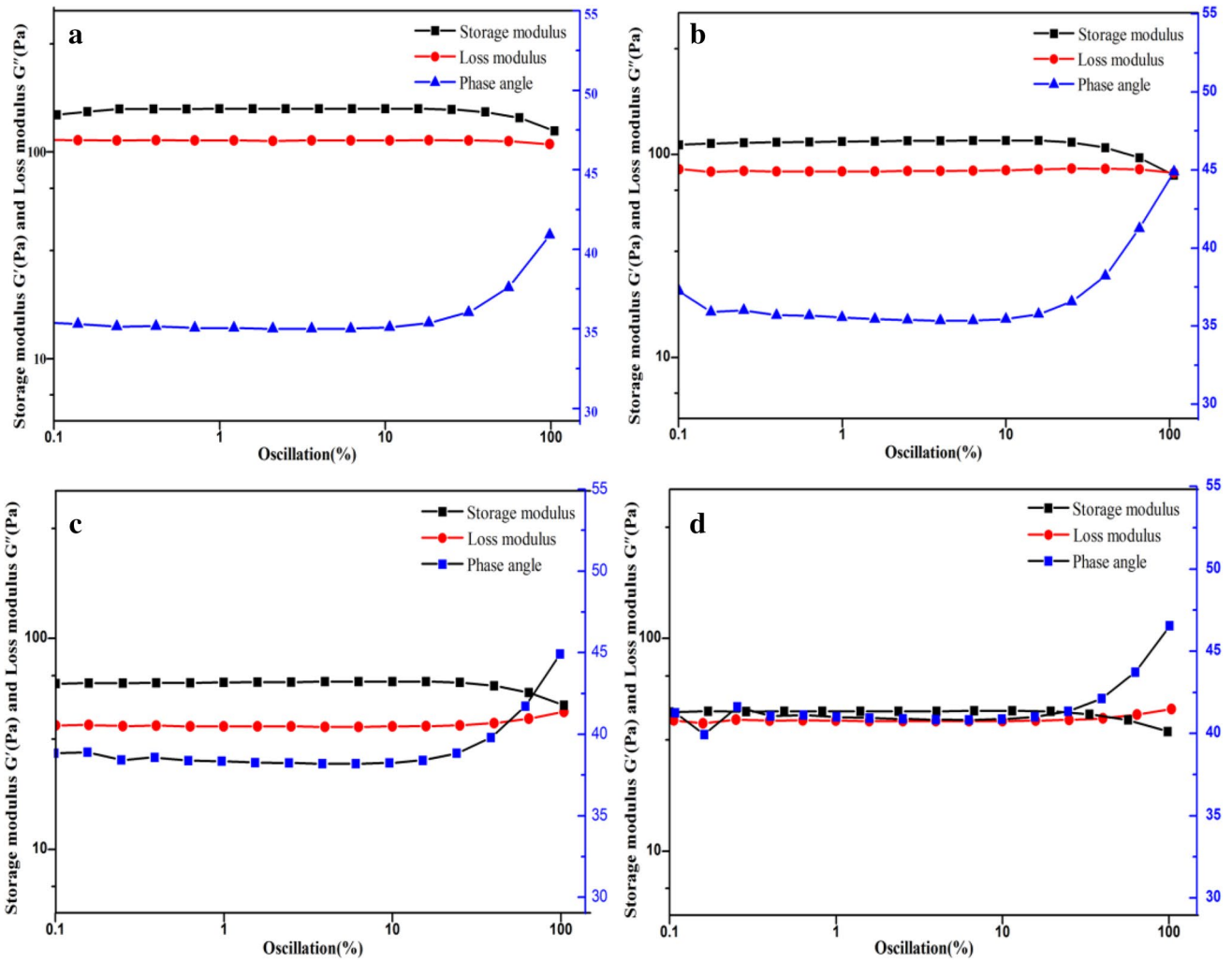

Fig. 8 Strain scans of PNIPA/HA composite hydrogels at 25 °C. **a** PNIPA/HA-2, **b** PNIPA/HA-3, **c** PNIPA/HA-4, **d** PNIPA/HA-5

interaction with nano-HA was weak. In the second region, both G' and G'' increased gradually with an increase of temperature and G' is largely higher than G''. This indicates that the elastic response of the material is stronger than the viscous response. When the temperature was higher than LCST, the hydrophobic of PNIPA was greatly enhanced, resulted more PNIPA molecules accumulating on the nano-HA through hydrogen bonding, exerting the bridging effect of nano-HA and increasing the modulus significantly. So the composite hydrogels displayed a predominantly solid-like behavior. The higher nano-HA content resulted the higher G' of PNIPA/HA-2 to PNIPA/HA-5. It might be attributed to the production of more hydrogen-bonding interactions.

3.6.3 Study on the Effect of Temperature on Viscosity

The composite complex viscosity of PNIPA/HA composite hydrogels under different temperatures have shown in Fig. 10. It can be seen that the composite viscosity does not changed obviously at lower temperatures. When the temperature was increased to 31.5 °C, the complex viscosity of the composite hydrogels in each group increased obviously. In addition, the amount of nano-HA had a great influence on the viscosity. With the increase of nano-HA content, the composite viscosity was increased more obviously with the increase of temperature.

3.6.4 Study on Flow Curve and Injectable Property

From Fig. 11, it can be seen that the viscosity of the PNIPA/HA composite hydrogels decreased with the shear rate increasing from 0.1 to 1000 s^{-1}. It indicates that the synthetic composite hydrogel was a non-Newtonian fluid with a shear thinning property, which was also an important requirement for injectable materials. With the increase of nano-HA content, the viscosity of PNIPA/HA composite

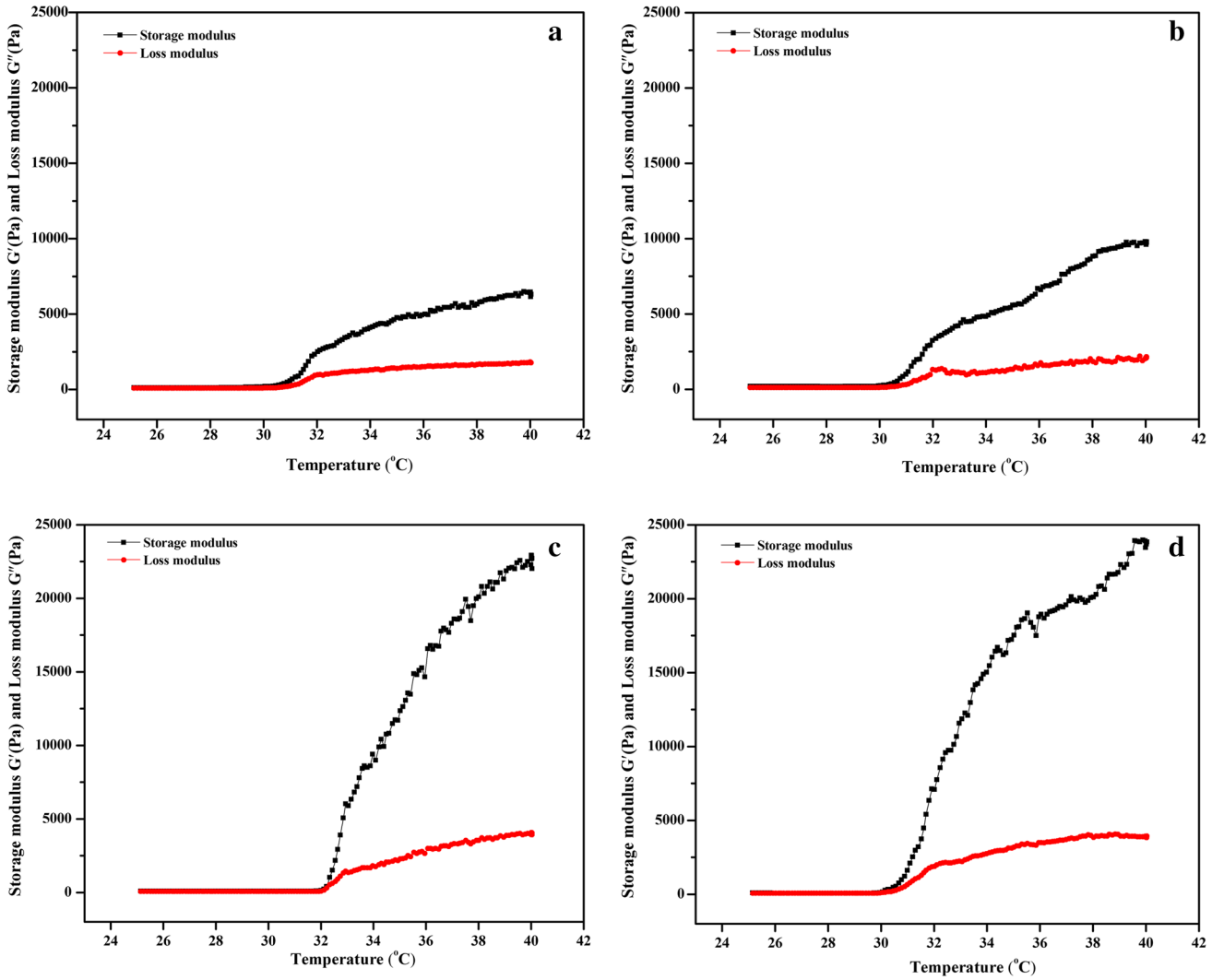

Fig. 9 Influence of temperature on the modulus of PNIPA/HA hydrogels. **a** PNIPA/HA-2, **b** PNIPA/HA-3, **c** PNIPA/HA-4, **d** PNIPA/HA-5

hydrogels decreased. So it could change the amount of nano-HA to control the viscosity of the composite hydrogels.

3.7 Swelling Studies

Swelling studies were carried out to further explore the influence of nano-HA content on the performance of PNIPA/HA composite hydrogels. Figure 12 has shown the swelling curves of all hydrogels with different nano-HA content. The swelling behaviors of PNIPA/HA composite hydrogels were studied at time interval of 1, 2–14 h. All hydrogels shows an increased swelling rate in the initial 5 h and then gradually flattened. With the increasing nano-HA content, the swelling rate decreases significantly. It can be seen that the equilibrium swelling ratio decreases from 2.25 to 1.66 when the nano-HA content increased from 2 to 5‰. It was speculated that the increase of the nano-HA content, made the internal network structure more compacted than that of the PNIPA/HA composite hydrogels, so it was difficult for water to enter and exit. These results demonstrated that the PNIPA/HA composite hydrogels exhibited a good water absorption capacity and the incorporation of nano-HA could influence the swelling behavior.

3.8 Hemolysis Assay

The thermosensitive PNIPA/HA composite hydrogels should be potentially used in tissue engineering field, so the hemocompatibility of the hydrogels was also studied. He [41], Golafshan [42] and others used similar test methods to evaluated their materials. Figure 13 is the photographs of hemolysis test. It can be clearly seen that there is no obvious difference in the appearance of the samples after incubation at 37 °C. When the samples were

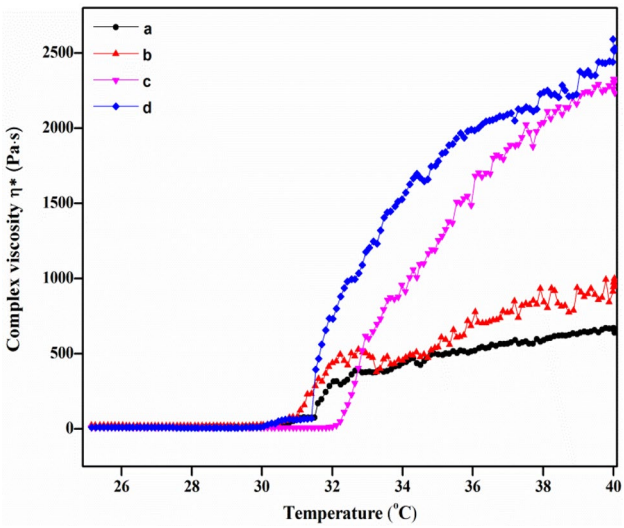

Fig. 10 Complex viscosity of PNIPA/HA hydrogels under different temperature. *a* PNIPA/HA-2, *b* PNIPA/HA-3, *c* PNIPA/HA-4, *d* PNIPA/HA-5

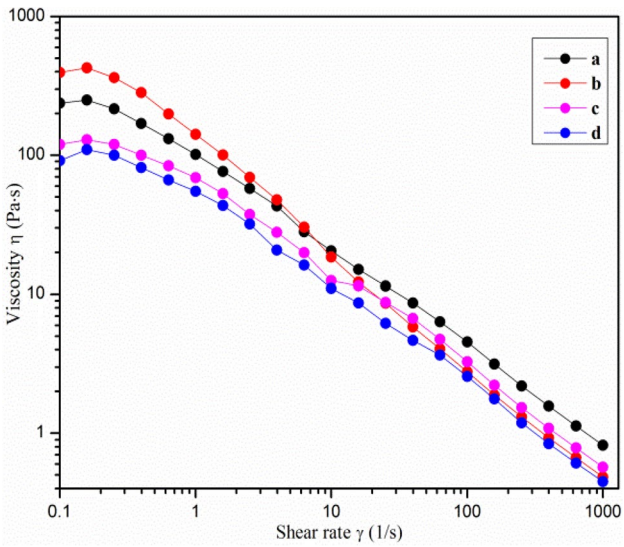

Fig. 11 Viscosity of PNIPA/HA hydrogels with the cutting speed. *a* PNIPA/HA-2, *b* PNIPA/HA-3, *c* PNIPA/HA-4, *d* PNIPA/HA-5

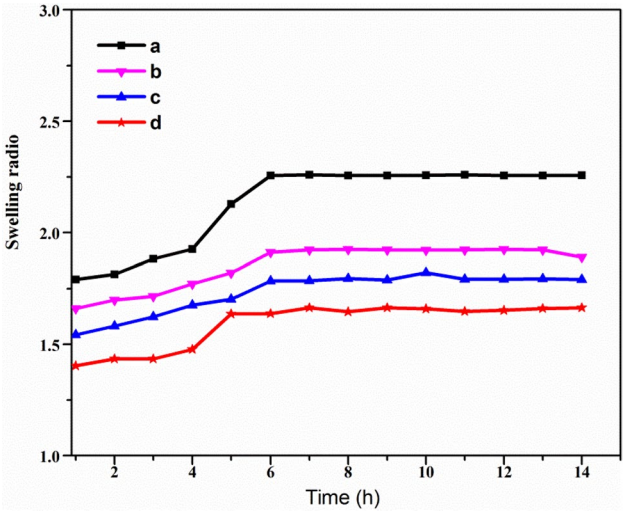

Fig. 12 Swelling studies of PNIPA/HA hydrogels. Swelling behavior of various hydrogels immersed in 0.9% NS at 37 °C. *a* PNIPA/HA-2, *b* PNIPA/HA-3, *c* PNIPA/HA-4, *d* PNIPA/HA-5

Fig. 13 Photographs of hemolysis test. The top figure shows the samples that were incubated at 37 °C, and the bottom figure shows the supernatant sample to be tested after centrifugation. The centrifuge tubes from the left to right are samples 1–6. Sample 1: the normal saline solution, samples 2–5: PNIPA/HA-2 to PNIPA/HA-5, sample 6: distilled water

centrifuged, the supernatant of the samples were different. The 0.9% NS solution was set as negative control 1% of hemolysis, while the distilled water was set as positive control with 100% of hemolysis. Theoretically, the samples were considered as toxic when having more than 5% hemolytic percentage [43]. As shown in Fig. 14, all the prepared PNIPA/HA composite hydrogels exhibited less than 1% hemolysis which was below the acceptable limit (5%). It could be concluded that the PNIPA/HA composite hydrogels have little hemolysis and are non-toxic materials.

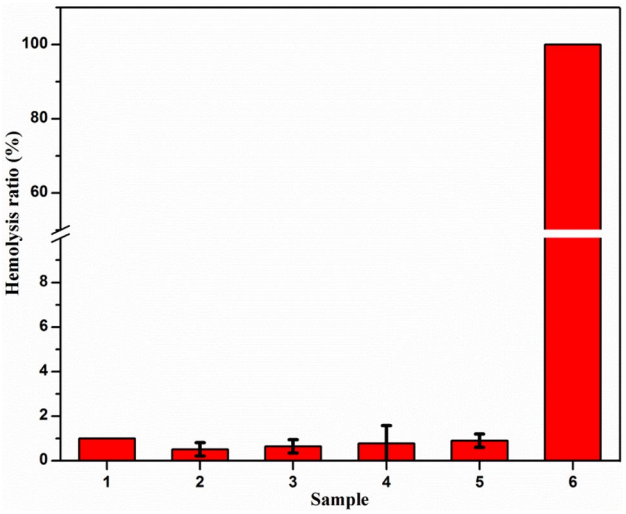

Fig. 14 Hemolysis test of PNIPA/HA hydrogels. Sample 1: the normal saline solution, samples 2–5: PNIPA/HA-2 to PNIPA/HA-5, sample 6: distilled water. To clearly show the low hemolysis of the experimental groups, the Y axis is presented in the style of "break"

4 Conclusions

PNIPA/HA organic–inorganic composite hydrogels were prepared by radical polymerization with nano-HA particles as a physical cross-linking agent, which avoided the use of chemical cross-linker. The prepared composite hydrogels had more hollow structures. Compared with PNIPA-0 hydrogel, the thermal stability of PNIPA/HA composite hydrogels has no significant changes. Besides, in composite hydrogels, the amount of nano-HA did not change the LCST, but increased modulus (especially the storage modulus) and viscosity significantly when the temperature was above the LCST. Good shear thinning characteristics and little hemolysis of these composite hydrogels were found.

Acknowledgements The author thanks Chunhui Li for his assistance in the assay of scanning electron microscopy and Xiaonan Dai for her technical assistance of rheological tests.

References

1. S.K. Katti, Colloids. Surf. B **39**, 133 (2004)
2. Y. Lei, Z.L. Xu, Q.F. Ke, W.J. Yin, Y.X. Chen, C.Q. Zhang, Y.P. Guo, Mater. Sci. Eng. C **72**, 134 (2017)
3. Y.G. Zhang, Y.J. Zhu, F. Chen, T.W. Sun, ACS Appl. Mater. Inter. **9**, 7918 (2017)
4. A. Manna, S. Pramanik, A. Tripathy, A. Moradi, Z. Radzi, B. Pingguanmurphy, RSC. Adv. **6**, 102853 (2016)
5. Y.F. Huang, J.Z. Xu, D. Zhou, L. Xu, B. Zhao, Z.M. Li, Compos. Sci. Technol. **151**, 234 (2017)
6. B.S. Kim, S.S. Yang, J. Lee, J. Biomed. Mater. Res. B **102**, 943 (2014)
7. A. Ficai, E. Andronescu, G. Voicu, C. Ghitulica, B.S. Vasile, D. Ficai, Chem. Eng. J. **160**, 794 (2010)
8. U.G. Wegst, H. Bai, E. Saiz, A.P. Tomsia, R.O. Ritchie, Nat. Mater. **14**, 23 (2015)
9. L. Jiang, Y. Li, C. Xiong, S. Su, H. Ding, ACS Appl. Mater. Inter. **9**, 4890 (2017)
10. B.H. Atak, B. Buyuk, M. Huysal, S. Isik, M. Senel, W. Metzger, Carbohyd. Polym. **164**, 200 (2017)
11. H. Wang, Y. Li, Y. Zuo, J. Li, S. Ma, L. Cheng, Biomaterials **28**, 3338 (2007)
12. R.L. Sala, M.Y. Kwon, M. Kim, Tissue Eng. A **23**, 935 (2017)
13. A. Ahiabu, M.J. Serpe, ACS Omega **2**, 1769 (2017)
14. C. Yang, Z. Liu, C. Chen, K. Shi, L. Zhang, X.J. Ju, W. Wang, R. Xie, L.Y. Chu, ACS Appl. Mater. Inter. **9**, 15758 (2017)
15. S.C. Grindy, N. Holten-Andersen, Soft Matter **13**, 4057 (2017)
16. M. Rizwan, G.S. Peh, H.P. Ang, N.C. Lwin, K. Adnan, J.S. Mehta, Biomaterials **120**, 139 (2016)
17. U. Bhutani, S. Majumdar, Mater. Discov. **8**, 1 (2017)
18. J.J. Kim, K. Park, Bioseparation **7**, 177 (1998)
19. P. Wang, Y. Zhang, L. Cheng, Macromol. Chem. Phys. **216**, 164 (2015)
20. Y. Qu, B.Y. Wang, B. Chu, C. Liu, X. Rong, H. Chen, J.R. Peng, Z.Y. Qian, ACS Appl. Mater. Inter. **10**, 4462 (2018)
21. T. Tanaka, Phys. Rev. Lett. **40**, 820 (1978)
22. H.Y. Liu, X.X. Zhu, Polymer **40**, 6985 (1999)
23. J.S. Scarpa, D.D. Mueller, I.M. Klotz, J. Am. Chem. Soc. **89**, 6024 (1967)
24. M. Heskins, J.E. Guillet, J. Macromol. Sci. A **2**, 1441 (1968)
25. K.S. Oh, J.S. Oh, H.S.C. And, Y.C. Bae, Macromolecules **31**, 7328 (1998)
26. D. Healy, M. Nash, A. Gorleov, K. Thompson, P. Dockery, Y. Rochev, Colloids. Surf. B **159**, 159 (2017)
27. E. Lai, Y. Wang, Y. Wei, G. Li, G. Ma, J. Appl. Polym. Sci. **133**, n/a (2016)
28. Z. Ding, Z. Fan, X. Huang, Q. Lu, W. Xu, D.L. Kaplan, ACS Appl. Mater. Inter. **8**, 24463 (2016)
29. S. Chen, J. Shi, X. Xu, J. Ding, W. Zhong, L. Zhang, Colloids Surf. B **140**, 574 (2016)
30. M. Annaka, T. Matsuura, M. Kasai, T. Nakahira, Y. Hara, T. Okano, Biomacromolecules **4**, 395 (2003)
31. F.K. Shi, M. Zhong, L.Q. Zhang, X.Y. Liu, X.M. Xie, Chin. J. Polym. Sci. **35**, 25 (2017)
32. J. Shan, M. Nuopponen, H. Jiang, E. Kauppinen, Macromolecules **36**, 4526 (2003)
33. H.H. Ren, H.Y. Zhao, Y. Cui, X. Ao, A.L. Li, Z.M. Zhang, Chin. Chem. Lett. **28**, 2116 (2017)
34. Y.M. Lee, H.M. Yun, H.Y. Lee, H.C. Lim, H.H. Lee, H.W. Kim, J. Biomed. Nanotechnol. **13**, 180 (2017)
35. J.F. Liao, B.Y. Wang, Y.X. Huang, Y. Qu, J.R. Peng, Z.Y. Qian, ACS Omega **2**, 443 (2017)
36. X.Z. Zhang, D.Q. Wu, C.C. Chu, Biomaterials **25**, 3793 (2004)
37. R. Freitag, F. Garret-Flaudy, Langmuir **18**, 3434 (2002)
38. P. Tempesti, G.S. Nicotera, M. Bonini, E. Fratini, P. Baglioni, J. Colloid Interf. Sci. **509**, 123 (2018)
39. H. Zhang, F. Li, B. Dever, C. Wang, X.F. Li, X.C. Le, Angew. Chem. Int. Ed. **52**, 10698 (2013)
40. X. Zou, X. Kui, R. Zhang, Y. Zhang, X. Wang, Q. Wu, P. Sun, Macromolecules **50**, 9340 (2017)
41. M. He, Q. Wang, R. Wang, Y. Xie, W. Zhao, C. Zhao, ACS Appl. Mater. Inter. **9**, 15962 (2017)
42. N. Golafshan, R. Rezahasani, E.M. Tarkesh, M. Kharaziha, S.N. Khorasani, Carbohyd. Polym. **176**, 392 (2017)
43. B. Iqbal, N. Muhammad, A. Jamal, P. Ahamd, Z.U.H. Khan, A. Rahim, J. Mol. Liq. **243**, 720 (2017)